The genesis of manganese deposits in the Ali Khanzai Block from the Zhob Ophiolite, Pakistan: Inferences from geochemistry and mineralogy

Journal:	*Journal of Earth Science*
Manuscript ID	JES-10-2019-0350.R3
Manuscript Type:	Original Article
Date Submitted by the Author:	n/a
Complete List of Authors:	Khan, Muhammad; University of Balochistan, centre of excellence in mineralogy; Kakar, M.Ishaq; University of Balochistan, Centre of Excellence in Mineralogy Ulrich, Thomas ; Department of Geoscience, Aarhus University, Høegh-Guldbergs Gade 2, DK-8000 Aarhus C, Denmark Ali, Liaqat; National Center of Excellence in Geology, University of Peshawar Kerr, Andrew; Cardiff University, Main Building, Park Place, Cardiff, Wales, CF10 3AT, UK., School of Earth and Ocean Sciences Mahmood, Khalid; Department of Earth Sciences, University of Sargodha Siddiqui, Rehanul; Balochistan University of Information Technology, Engineering and Management Sciences
Keywords:	mineral, Deposit, geology

The genesis of manganese deposits in the Ali Khanzai block of the Zhob Ophiolite, Pakistan: Inferences from geochemistry and mineralogy

Muhammad Ayoub Khan[1], Muhammad Ishaq Kakar[1], Thomas Ulrich[2], Liaqat Ali[3], Andrew C. Kerr[4], Khalid Mahmood[5], Rehanul Haq Siddiqui[6]

[1]*Center of Excellence in Mineralogy, University of Balochistan, Quetta, Pakistan*

[2]*Department of Geoscience, Aarhus University, Høegh-Guldbergs Gade 2, DK-8000 Aarhus C, Denmark*

[3]*National Center of Excellence in Geology, University of Peshawar, Peshawar, Pakistan*

[4]*School of Earth and Ocean Sciences, Cardiff University, Main Building, Park Place, Cardiff, Wales, CF10 3YE, UK*

[5]*Department of Earth Sciences, University of Sargodha, Sargodha, Pakistan*

[6]*Balochistan University of Information Technology, Engineering and Management Sciences, Quetta, Pakistan*

Corresponding Author Email: ayoub.cemuob@gmail.com

Abstract

The Zhob Ophiolite comprises the Naweoba, Omzha and Ali Khanzai blocks, which are surrounded by the sediments of the Alozai Group and Loralai Formation. The Ali Khanzai block contains metamorphic, ultramafic, gabbroic, volcanic and volcaniclastic rocks with associated chert. The Zhob manganese deposits found in the Ali Khanzai block, occur in banded, lenticular and massive forms within red to brown coloured metachert. Braunite and pyrolusite are the main constituent manganese-bearing minerals with minor hausmannite, hematite and barite while quartz is the major gangue mineral with some carbonate minerals. Geochemical evidence from the major oxides indicates that the manganese mineralization and

associated metachert at Zhob were formed by hydrothermal activity with little contribution from contemporaneous volcanic materials and this is confirmed by high Fe/Mn and low Co/Zn ratios and trace element patterns. These deposits formed along with seafloor spreading centres and were later obducted as part of Ali Khanzai block of Zhob Ophiolite.

Key Words: Zhob Ophiolite, Manganese ore, Hydrothermal, Genesis

1. Introduction

Manganese deposits occur in a range of tectonic settings, with ore deposits being associated with ophiolites as well as continental sedimentary sequences. These deposits can be divided into three types based on mineralogy, geochemical composition and tectonic setting: 1) hydrogenous, 2) hydrothermal, and 3) diagenetic/biogenetic-bacterial deposits (Polgari et al., 2012; Oksuz, 2011; Hein et al., 1997; Bolton et al., 1988). Hydrogenous deposits occur as ferromanganese crusts which are slowly precipitated (2–10 mm/Ma) from seawater on the seafloor usually via microbial mediation and are usually depleted in Mn minerals and rich in amorphous iron compounds (Oksuz, 2011; Jach and Dudek, 2005; Usui and Someya, 1997; Toth, 1980). Hydrogenous deposits are characterized by a low Mn/Fe ratio (~1) and high trace element concentrations, particularly Ni and Cu (Usui and Someya, 1997; Hein et al., 1996, 1997; Usui and Nishimura, 1992; Ingram et al., 1990; Toth, 1980;).

In contrast, hydrothermal deposits precipitate directly from low-temperature hydrothermal solutions (Hein et al., 1997; Ingram et al., 1990) and are commonly stratabound and laminated or occur as irregular bodies and epithermal veins. They are found in modern and ancient environments in marine settings adjacent to either spreading centres or intraplate seamounts, or subduction-related island arc settings (Roy, 1992, 1997). Diagenetic or bacterial deposits are mainly found as nodules and precipitate from hydrothermal solutions or pore

waters. These manganese deposits are generally related to oxidation of organic matter and formation of Mn-carbonate mineralization (Oksuz, 2011; Polgári et al., 1991, 2012), however, they can also form by a combination of these processes. Unlike hydrogenous deposits, hydrothermal and diagenetic deposits have high Mn/Fe ratios and low trace metal contents (Hein et al., 1994, 1996). Although diagenetic and hydrothermal deposits are similar in some ways, these two types can be distinguished on the basis of their morphology, tectonic setting and growth rates (Kuhn et al., 1998).

In Pakistan, manganese deposits are reported mainly from North Waziristan, Lasbela, Kurram, Bajaur, Mohmand, and Mansehra. All the manganese deposits are associated with ophiolitic rocks except that of Mansehra, which is hosted by a continental sedimentary sequence (Asif, 2014; Shah and Moon, 2004; Shah and Khan, 1999; Naseem et al., 1997; Ahmed, 1992). Among these deposits, the North Waziristan (45 wt. % MnO), Lasbela (40 wt. % MnO) and Bajaur manganese (55.39 wt. % MnO) deposits are economically significant due to their grade and accessibility (Asif, 2014; Shah and Khan, 1999; Naseem et al., 1997).

The Zhob Ophiolite, in the Zhob valley, is located north-northeast of the Muslim Bagh Ophiolite (Fig.1b) and hosts several types of economic deposits including manganese ores (Ahmed, 1969, 1975; Bilgrami, 1964a, b; Jones, 1961; Heron and Crookshank, 1954). The manganese deposits in this study are located in the Ali Khanzai block of the ophiolite which is situated 16 km south of Zhob city (Fig.1c). This Zhob manganese occurrence was first reported by Ahmed (1975), who described the manganese occurring in the form of veins and layers, associated with basalt and chert. The Zhob manganese is being commercially mined since the deposits contain an average 42.5 wt. % MnO. In the current study, we present the first petrographic descriptions, mineralogy, and geochemistry of the Zhob manganese ores found associated with the Ali Khanzai block of the Zhob Ophiolite and propose a model for its paragenesis.

2. Regional Geology and Zhob Ophiolite

The Zhob Ophiolite is exposed in northwestern Pakistan and is part of the suture zone marked by the Bela, Muslim Bagh and Waziristan ophiolite complexes (Sengor, 1987; Fig. 1a). In the south, the rocks of the suture zone are thrusted over the Calcareous zone, which is comprised of a marine succession (Triassic-Jurassic) of the Sulaiman Fold-Thrust Belt. In contrast, in the north, the rocks of the suture zone are overlain by the Pishin-Katawaz flysch succession, comprising the Nisai (Eocene) and Khojak Formations (Oligocene) (Fig. 1b). The rock units in immediate contact with the Zhob Ophiolite include the Jurassic Alozai Group (Durrani, 2012) at the base, and the Nisai Formation (Eocene-Oligocene; Bukhari et al., 2016) at the top.

The Zhob Ophiolite consists of three separate blocks; the Naweoba, Omzha and Ali Khanzai blocks. These blocks contain metamorphic rock, serpentinized peridotite, mafic oceanic crustal rocks, basaltic volcanic rocks and sedimentary rocks such as chert and mudstone. These blocks contain a few narrow elongated bodies of diorite parallel to peridotite and volcanic rocks.

3. Geology of the Ali Khanzai block and manganese ore deposits

The Ali Khanzai block is approximately 12 km long and up to 3 km wide, and is located about 16 km to the south of Zhob city (Fig. 1c). The Ali Khanzai block consists of metamorphic rocks, a mantle section, mafic oceanic crustal rocks and a basalt-chert unit (Fig. 1c; Rehman, 2019). The contacts between various rock units of the Ali Khanzai block are sharp and sometimes irregular because it is tectonically disturbed (Rehman, 2019). Sub-ophiolitic metamorphic rocks found beneath the mantle section are mostly amphibolites, greenschists and mica schist. The mantle section is fragmented and distributed across the base of this block and is composed of dunite and harzburgite which are highly serpentinized. The crustal section

contains mainly layered and massive gabbros and some doleritic dykes which are quite deformed and tectonically disturbed. The volcanic-chert-unit is the largest unit of Ali Khanzai block and comprises volcanic rocks, volcaniclastic rocks and metachert. Basalt is a significant volcanic rock and occurs commonly in pillow and sheet forms. These units cannot be stratigraphically correlated across the Ali Khanzai block due to intense folding, faulting and the exotic nature of the rocks in the block.

Chert in the volcanic-chert-unit is highly folded, fractured and metamorphosed, and hosts manganese mineralization. These metacherts are fine-grained and crystalline and are thin to medium-bedded. They have gradational contacts with underlying volcanic rocks and are interbedded with volcanic rocks in some localities. The metacherts of the Ali Khanzai block are cryptocrystalline and comprise fine-grained quartz along with minor clay minerals and mainly consist of non-detrital free silica. Occasionally the metachert contains radiolarian tests that are filled with detrital quartz and clay minerals.

Manganese mineralization in the Ali Khanzai block is identified by its black colour in the field (Fig. 2). Manganese deposits are scattered (50 to 100 meters apart) and occur as small deposits associated with reddish-to-brown metachert of the basalt-chert-unit of the Ali Khanzai block (Fig. 1c). These deposits are collectively described here as the Zhob manganese deposits and are currently being explored and mined, however the actual size of these manganese deposits remains unknown.

The ore deposits in the investigated area are scattered and irregular but conformable with their host rocks. They lie above the volcanic rock-chert unit and are associated with reddish-to-brown metachert. The ore deposits occur at a variable distance from the boundaries between metachert and volcanic rocks. The thickness of the ore bodies varies from 1 cm to 200 cm, they are separated by layers of reddish-to-brown metachert. The general trend of the mineralization is SW-NE and is consistent with the bedding of the host rock. Manganese ores

and host rocks are folded, faulted and fragmented, indicating that considerable deformation occurred after the formation of the deposits. These ore deposits occur in layered, banded, lenticular and massive forms (Fig.2). The lenticular and layered ore bodies are surrounded by metacherts (Fig. 2a-b). The banded form of manganese, containing Mn-rich phases, are thin to medium in size and are clearly visible and alternate with bands of the host the metachert (Fig. 2c). Massive manganese is very thick and irregular (Fig. 2d) and has sharp contacts with the host metacherts. The pockets of manganese ore are enveloped by the surrounding host rock and are disconnected and rounded to subrounded.

4. Samples and analytical methods

Around 60 samples of massive, layered and banded ores and metachert (host rocks) were collected in the field. These samples of ores and metachert were studied petrographically. The least-altered 13 samples of ores and 7 samples of metachert were selected for major and trace element analysis. Fe_2O_3, MnO, MgO, CaO, Na_2O, TiO_2 and K_2O were determined by atomic absorption spectrometry (Perkin Elmer 3300, equipped with graphite furnace), while SiO_2, P_2O_5 and Al_2O_3 were analysed by a Pye Unicam UV/visible spectrophotometer (detailed methodology and standards are in Appendix; supplementary material). The trace elements such as Cu, Pb, Zn, Ni, Cr, and Co were also determined by the Atomic Absorption Spectrometry (detailed methodology and standards are in Appendix; supplementary material). The loss on ignition (L.O.I.) was determined by heating the samples at 1000 °C in a muffle furnace.

Petrographical and mineralogical studies were carried out using both polarized and reflected light microscopy of polished thin sections. All of the above studies were carried out at the Geochemistry Laboratory of the National Centre of Excellence in Geology, University of Peshawar, Pakistan.

The mineralogical studies of ore and gangue minerals are based on a combination of X-ray powder diffraction analysis (XRD Bruker D-8 Advance with Cu anode operating at a generator voltage of 40 kV) and ore microscopy at Center of Excellence in Mineralogy, University of Balochistan, Quetta, Pakistan.

The qualitative phase composition of the ore and gangue minerals were analysed by Micro X-ray fluorescence spectroscopy (μ-XRF) using polished blocks of the representative samples. The X-ray fluorescence analysis was conducted on a Bruker M4 Tornado X-ray machine at the Institute of Geoscience at Aarhus University, Denmark. The source used was a single rhodium target X-ray tube. All samples were scanned using the same parameters. The spot size was 20μm and the distance between measured points was 25μm. Two spectrometers were operated at a range of 40 keV / 130 kcps. The X-ray tube was run at 50kV electron voltage and the current was set to 600μA. All analyses were carried out in a vacuum.

Quantitative mineral chemistry of manganese minerals was analyzed at the Department of Geoscience, Aarhus University, Denmark, using a JEOL JXA-8600 electron microprobe equipped with EDS (energy dispersive x-ray spectroscopy) with an acceleration voltage set to 15KeV and a current beam of 10nA. The beam diameter was 5 μm with a counting time of 20 seconds. For the calibration of the microprobe natural mineral standards were used. The analysis quality was monitored with two in-house standards; clinopyroxene BB1 and labradorite (Oslo plagioclase). These standards were measured intermittently and compared with the known composition to check the quality of the analysis. Carbon-coated polished thin sections were used for this analysis.

5. Mineralogy and petrography of manganese ore

X-Ray diffraction has determined that braunite and pyrolusite are the most dominant Mn-minerals with associated minor hausmannite, hematite and barite while quartz is most the

common gangue mineral. Braunite is the principle manganese mineral and it ranges in shape from microcrystalline to coarse-grained and anhedral to subhedral. Microcrystalline braunite is intermixed with microcrystalline to cryptocrystalline quartz while the coarse-grained braunite grains are interlocked with each other and are occasionally cross-cut by veinlets of quartz (Fig. 3a). Coarse-grained braunite usually occurs as a homogeneous mass but is also found as a rim around pyrolusite (Fig. 3b). Pyrolusite occurs as massive anhedral to subhedral grains as well as disseminated grains in Mn minerals and gangue minerals and it can also fill cracks and spaces between minerals. It is also found in micro-veins formed by filling of fractures and cracks in braunite and gangue minerals particularly cryptocrystalline quartz (Fig. 3c). Massive pyrolusite grains show needle, flake and fibrous shapes (Fig. 3d). Breccia-like textures between pyrolusite and quartz are also common.

Hematite is associated with Mn minerals and occurs as a fine-grained matrix (Fig. 3b) enclosing Mn minerals and forms veins along with gangue minerals. Hematite also occurs as finely disseminated grains together with microcrystalline Mn minerals and cryptocrystalline quartz. Gangue minerals are predominantly quartz and carbonate with minor barite. Quartz is usually crushed due to deformation and is cryptocrystalline to microcrystalline. It occurs as veinlets and well-developed crystals, filling vugs or interstitial spaces of manganese and iron minerals (Fig. 3e). Carbonate is mainly calcite that commonly forms irregular or sometimes oval patches and fills the veins and cracks within manganese and iron oxide matrix. Barite is very rare and fills cavities in manganese-rich phases (Fig. 3f).

Hence, three stages of mineralization are recognized in Zhob manganese mineralization including; early, middle, and late stages. The early stage is represented by massive pyrolusite minerals, while the middle stage is characterized by braunite with replacement textures and enclosing pyrolusite. Late-stage supergene mineralization

comprising pyrolusite, hematite and barite minerals are found infilling fractures and fissures (Fig. 4).

6. Geochemistry

6.1. Mineral chemistry

Compositions of the main minerals identified in the Zhob manganese ore are given in Table 1. Braunite is one of the most significant manganese ore minerals and it normally contains up to 10 wt. % SiO_2 (Roy, 1981). However, in silicate-rich braunite SiO_2 contents can be up to 40%, depending on temperature and partial oxygen pressure during formation (Maun, 1959; Naseem, 1996). The studied ore from the Ali Khanzai block contains both normal braunite and silicate-rich braunite. The average composition of normal braunite is SiO_2 (13.0 wt. %), Al_2O_3 (1.5 wt. %), Fe_2O_3 (1.1 wt. %), Mn_2O_3 (82.9 wt. %), MgO (0.3 wt. %) and CaO (1.45 wt. %) while silicate-rich braunite contains SiO_2 (28.4 wt. %), Al_2O_3 (1.2 wt. %) and MnO (67.5 wt. %).

Pyrolusite is also a dominant mineral in the Zhob deposits with a typical composition of 98.3 wt. % MnO_2 and 0.90 wt. % Fe_2O_3. The low totals indicate the presence of some absorbed water in the pyrolusite (Gutzmer and Beukes, 1997; Frenzel, 1980).

Hematite is an accessory mineral and its composition averages 89.7 wt. % Fe_2O_3, 9.1 wt. % Mn_2O_3 and 1.6 wt. % TiO_2. However, the high contents of Mn_2O_3 suggest that hematite may have incorporated Mn into its structure from the coexisting Mn-phases during metamorphism (Shah and Moon, 2004).

The few grains of barite that have been observed have an average composition of 70.0 wt. % BaO, 27.1 wt. % SO_3 and 0.9 wt. % SrO. Small amounts of FeO, CaO and MnO in the barite composition may have been substituted for BaO.

6.2. Whole Rock Geochemistry

The whole-rock composition of manganese ores and host rocks of the studied deposits are given in Tables 2 and 3, respectively. Manganese ore samples have been divided into Mn-rich and Fe-rich manganese ores. Average major elements contents (wt. %) of Mn-rich and Fe-rich manganese ore samples and their host rocks are compared in Fig. 5a. Mn-rich ores are higher in MnO and lower in Al_2O_3, Fe_2O_3 and SiO_2 than Fe-rich ores. Host rocks are much higher in SiO_2 than manganese ores while almost similar in the other major elements to the manganese ores.

Trace element concentrations (ppm) of Mn-rich and Fe-rich manganese ores and their host rocks are compared in Fig. 5b. Fe-rich manganese ores are higher in Pb, Co, Ni, Zn and Cu and more depleted in Cr than the Mn rich ores. Trace element contents in the host rocks are much lower than in the manganese ores except for Cu and Cr which are broadly the same. The samples of Fe and Mn-rich ores will be discussed together in the following section because they have been sampled from the same deposits.

7. Discussion

The common veining, brecciation, mesh textures and crushed grains of ore and gangue minerals of Zhob manganese deposits reveal that after their formation, the rocks of the studied area may have undergone regional metamorphism (see Gutzmer and Beukes, 1997; Ostwald and Nayak, 1993; Roy et al., 1990; Abs-Wurmbach et al., 1983; Dasgupta and Manickavasagam, 1981; Roy, 1981). The mesh texture, in which pyrolusite is surrounded by braunite, indicates the replacement of pyrolusite by braunite and suggests that braunite was formed due to the reaction between pyrolusite (early formed phase) and iron-oxide (hematite) and subsequent recrystallization and remobilization caused incorporation and readjustment of Mn, Fe, Si, P, Al and Pb from pyrolusite, hematite, quartz, and barite (Shah and Moon, 2004).

The occurrence of pyrolusite as relics within braunite confirms this inference. However, the presence of pyrolusite as fracture-filled micro-veins could also be related to supergene enrichment (Shah and Moon, 2004). Braunite is a characteristic mineral of greenschist to granulite facies conditions (Gutzmer and Beukes, 1997; Abs-Wurmbach et al., 1983; Roy, 1981). Hence, the mineralogy and texture of the minerals found in the Zhob manganese ores support the idea that rocks of the area have been locally subjected to greenschist facies metamorphism.

The major oxides SiO_2, Fe_2O_3, MnO, Al_2O_3 and TiO_2 and trace element contents as well as ratios of major and trace elements are useful in assessing the paragenesis of manganese ore deposits (Zarasvandi et al., 2013; Polgari et al., 2012; Karakus et al., 2010; Shah and Khan, 1999; Crerar et al., 1982).

The Si vs. Al binary discrimination diagram proposed by Toth (1980) and Peters (1988), is widely used to assess the hydrothermal, sedimentary or hydrogenous (i.e., from seawater deposition) origins of manganese mineralization (Oksuz, 2011; Karakus et al., 2010; Mücke et al., 1999; Nicholson, 1992). SiO_2 concentration is typically high in hydrothermally-formed sediments as compared with hydrogenous deposits (Karakus et al., 2010). Almost all the samples from the Zhob deposits plot within the field of hydrothermal deposits similar to the Waziristan (Pakistan) and Dehoo (Turkey) manganese deposits (Fig. 6a). In addition to the hydrothermal processes, other processes and components such as diagenesis, clastic materials, and biosilica can increase the Si concentrations (e.g., Polgári et al., 2012; Toth, 1980).

The triangular plot of Mn-Fe-(Co+Ni+Cu) ×10 (Hein et al., 1992; Crerar et al., 1982; Toth, 1980; Bonatti, 1972) has also been successfully used to help distinguish manganese mineralization of various origins. The Zhob ores again plot in the hydrothermal field (Fig. 6b) almost identical to Waziristan (Pakistan) and Dehoo (Turkey) manganese deposits. The Zn-Ni-Co triangular diagram (Choi and Hariya, 1992) also shows the hydrothermal origin of Zhob

deposits (Fig. 7a) and illustrates that they are compositionally similar to other hydrothermal manganese deposits like those in Waziristan (Pakistan) and Dehoo (Iran). The Co/Zn vs. Co+Ni+Cu diagram (Toth, 1980), once again reveals the hydrothermal genesis of the Zhob deposits (Fig. 7b).

Mn/Fe ratio is used to delineate the origin of manganese deposits; for example, for lacustrine deposits (Mn/Fe < 1), hydrogenous deposits (Mn/Fe = 1), SEDEX deposits (0.1 <Mn/Fe < 10) (Nicholson et al., 1997) while a high Mn/Fe ratio is characteristic of hydrothermal deposits (Jach and Dudek, 2005). The Mn/Fe ratios of the Zhob manganese deposits range from 1.7 to 561 (mean 106). The available average Mn/Fe ratios of world manganese deposits are as follows: Waziristan - 199 (Shah and Khan, 1999), Cayirli - 97 (Karakus et al., 2010), Dehoo - 80 (Lotfi, 2017), Hazara - 2 (Shah and Moon, 2004), Eymir - 880 (Oksuz, 2011), Nasirabad – 19 (Zarasvandi et al., 2013), Buyukmahal - 48 (Oskuz and Okuyucu, 2014), Binkilic - 15 (Gultekin, 1997), Ulukent - 19, (Ozturk,1993) and Hinode - 133 (Choi and Hariya,1992). The comparison of the world manganese deposits is shown in Table 4. Among these deposits Waziristan, Cayirli and Dahoo are hydrothermal exhalative manganese deposits associated with ophiolites. The Hazara, Nasirabad, Buyukmahal, and Eymir deposits are of hydrothermal- hydrogenous origin while Binkilic, Ulukent, and Hinode deposits are formed in hydrogenous environments. Thus, the range of Mn/Fe ratio (1.7 to 561; avg. 106) of the Zhob manganese ore deposit is consistent with those of hydrothermal exhalative manganese deposits.

The behavior of Co and Ni are closely related to each other and are also closely associated with Mn oxides. On average, cobalt abundances decrease from hydrogenous to diagenetic and to hydrothermal manganese deposits (Zarasvandi et al., 2013; Sabatino et al., 2011). Deposits with Co/Ni < 1 are characteristic of sediments deposited in hot water (Fernandez and Moro, 1998) whereas Co/Ni > 1 indicates a deep marine environment of

formation (Toth, 1980). Apart from one sample, Co/Ni ratios in the Zhob manganese ore deposit are lower than 1 suggesting a sedimentary contribution to the mineralization (Table 2). Co/Zn ratios of ~0.15 are characteristic of hydrothermal manganese ore deposits while a ratio of ~2.5 indicates a hydrogenous origin for a manganese ore deposit (Toth, 1980). Co/Zn ratio for the Zhob manganese deposits ranges from 0.13 to 0.9 and indicates a hydrothermal origin for the manganese mineralization. These values are similar to the Waziristan manganese deposit and Dehoo ore deposit (Table 4). Although Co/Zn ratios suggest a hydrothermal origin for the Zhob ore deposits, Co/Ni ratios indicate a small contribution from a sedimentary component during the formation of the manganese deposits.

Like Fe and Mn values, concentrations of Ti and Al are also useful for the assessment of the genesis of Mn ore deposits. Al and Ti contents are high in the sedimentary environment and they have the same behavior during the formation of an ore deposit (Sugisaki, 1984; Crerar et al., 1982). Detrital materials are an important source of Al in the chemical precipitates of manganese ores (Zarasvandi et al., 2013; Polgari et al., 2012; Maynard, 2010), while titanium is essentially constant in hydrothermal solutions and is thus a measure of clastic (detrital) input (Şaşmaz et al., 2014; Shah and Khan, 1999; Sugisaki, 1984). The contents of Al and Ti in the Zhob deposits show a positive correlation (Fig. 7c) except for one sample which has markedly high Al_2O_3, probably due to alteration. This broad positive correlation, therefore, supports the contribution of detrital material in the formation of the deposits.

7.1. Genetic model of Zhob manganese deposits

The Zhob Ophiolite is part of the Bela-Zhob-Waziristan ophiolitic belt (Sengor, 1987). Ophiolites of this belt were obducted on the western margin of the Indian continental plate as the oceanic crust of Neo-Tethys Ocean and formed in a supra-subduction zone environment in Late Cretaceous (Kakar et al., 2014; Mahmood et al., 1995; Sawada et al., 1995). The Ali

Khanzai block of Zhob Ophiolite was the part of the crust Neo-Tethys ocean that contains manganese mineralization associated with metachert. By considering the models of Bonatti et al. (1976), Canon and Force (1983) and Buhn et al. (1992), a simple genetic model can be proposed for the origin of the Zhob manganese deposits (Fig. 8). The downward circulation of seawater into the fractured oceanic crust and interaction of the seawater with hot oceanic crust caused progressive warming and reduction and increase in the acidity that generated hydrothermal solutions (Roy, 1992). These solutions were able to leach Mn, Fe and other metals from the basaltic oceanic crust. Finally, the metal-enriched hydrothermal solutions convected upward to the seafloor lead the deposition of manganese and ferromanganese deposits.

The precipitation of different metals from the hydrothermal solutions are the result of decreasing pressure and temperature and increasing Eh and/or pH in the solution. Cooling of the hydrothermal solution may occur during circulation through cooler rocks and/ or by subsurface mixing with seawater. The origin of the Zhob manganese deposits similar to those of present-day hydrothermal systems within mid-oceanic spreading centers (Shah and Khan 1999; Roy, 1992). The formation of these deposits can be related to the Neo-Tethys Ocean where these deposits originated along with sea-floor-spreading centres and were later obducted as part of Zhob Ophiolite. During obduction, the Zhob Ophiolite has undergone metamorphism which may have caused alteration of the manganese deposits.

It is now understood that Fe compounds are less stable compared to Mn and so precipitate close to hydrothermal vents. Conversely, Mn is more stable in aqueous solution and so precipitates further away from hydrothermal vents at sea floor spreading centers (Roy, 1992; Panagos, 1984). The precipitation of Mn and Fe and their compounds are controlled by Eh and/or pH of the hydrothermal solution (Frakes and Bolton, 1992; Panagos, 1984). In low Eh and/or pH conditions Mn is more mobile relative to Fe. The fractionation of Mn compounds

from Fe compounds suggests a spatial variation in Eh and/or pH (Panagos, 1984). Considering Fe and Mn concentrations of mineralization in the study area, it is likely that the Zhob deposits were formed from a hydrothermal source and the high Fe contents, indicate that mineralization was probably proximal to a hydrothermal vent at a sea floor spreading center.

It is clear from the geochemical data in Figs. 6 and 7, and low Mn/Fe ratios (Table 3) of the host rocks (metachert) that metachert was formed by hydrothermal processes with a limited contribution from sedimentary (contemporaneous volcanic) components. The conformable nature of the Zhob manganese deposits and host metachert indicate that Mn and Si were probably both derived from the same hydrothermal source. Metachert contains radiolarian tests and this suggests that the metachert is formed from a mixture of biogenic and hydrothermal sediments.

8. Conclusions

The Zhob manganese ore deposits are hosted by red to brown metachert in the Ali Khanzai block of the Zhob Ophiolite. Braunite and pyrolusite are the main manganese minerals that occur together with minor hematite and barite. Gangue minerals are mainly quartz and carbonate minerals. Major and trace element signatures show that hydrothermal processes were responsible for the formation of mineralization at Zhob with a minor contribution from deterital (contemporaneous volcanic) materials. Therefore, it is concluded that the Zhob manganese deposits are hydrothermal in origin.

Acknowledgements

This research was financially supported by the six months, HRD Foreign scholarships of the Centre of Excellence in Mineralogy, University of Balochistan, Quetta, which was approved by the Higher Education Commission, Pakistan under its PSDP development project

"Capacity Building and Strengthening of the Centre of Excellence in Mineralogy". The research was also partly supported by Higher Education Commission, Pakistan "National Research Program for Universities (NRPU) Project # 3593" to M. Ishaq Kakar. The authors are grateful to the reviewers for their constructive comments which improved the manuscript.

References

Abs-Wurmbach, I., Peters, T. J., Langer, K., and Schreyer, W., 1983. Phase relations in the system Mn–Si–O and experimental and petrological study. *Neues Jahrbuchfür Mineralogie - Abhandlungen,* 146: 258–279

Adachi, M., Yamamoto, K., and Sugisaki, R., 1986. Hydrothermal chert and associated siliceous rocks from the northern Pacific: their geological significance as indication of ocean ridge activity. *Sedimentary Geology*, 47:125–148

Ahmed, Z., 1969.Directory of mineral deposits of Pakistan. *Geological Survey of Pakistan Record,* 15 (3):2000

Ahmad, Z., 1975. Geology and Petrochemistry of a part of the Zhob Valley Igneous Complex, Balochistan, Pakistan. *Geological Survey of Pakistan Record,* 24: 1-35.

Ahmed, Z., 1992. Manganese occurrences in ophiolitic rocks of Khuzdar district, Pakistan. *Acta Mineralogica Pakistanica,* 6: 65–73

Asif, M., 2014. Mineralogy, geochemistry and genesis of manganese deposit of Takht area, Bajaur Agency, NW Pakistan: [Dissertation]. University of Peshawar, Peshawar. 86.

Bannert, D., Cheema, A., and Ahmad, A., 1992. The geology of the Western Fold Felt: Structural interpretation of the Landsat-MSS Satellite Imagery 1:500,000. Federal Institute of Geosciences and Natural Resources, Han., Germany.

Bilgrami, S. A., 1964a. Mineralogy and petrology of the central part of the Hindubagh igneous complex, Hindubagh mining district, Zhob Valley, West Pakistan. *Geological Survey of Pakistan Record*, 10: 28

Bilgrami, S. A., 1964b. Regional distribution of the chemically different chromites from Zhob Valley, West Pakistan. *Geological Bulletin Punjab University*, 4:1-16

Bolton, B. R., Bot, R., Exon, N. F., Hamilton, T. F., Ostwald, J., and Smith, J. D., 1988. Geochemistry and mineralogy of sea floor hydrothermal and hydrogenetic Mn oxide deposits from the Manus Basin and Bismarck Archipelago region of the southwest Pacific Ocean. *Marine Geology,* 85:65–87

Bonatti, E., Kraemer, T., and Rydell, H., 1972. Classification and genesis of submarine iron-manganese deposits. In: Horn, D. R., (Ed). Ferromanganese Deposits of the Ocean Floor. National Science Foundation, Washington, DC, pp 149–166

Bonatti, E., Zerbi, M., Kay, R., and Rydell, H., 1976. Metalliferous deposits from the Apennine ophiolites: Mesozoic equivalents of modern deposits from oceanic spreading centres. *Geological Society of American Bulletin, 87*: 83–94

Buhn, B., Stanistreet, I. G., and Okrusch, M., 1992. Late Proterozoic outer shelf manganese and iron deposits at Otjosondu (Namibia) related to the Damaran oceanic opening. *Economic Geology, 87:* 93–144

Cannon, W. F., and Force, E. R., 1983. Potential for high-grade shallow marine manganese deposits in North America. In: Shanks, W. C III (ed) Cameron volume on unconventional mineral deposits. New York Society Mining Engineers/American Institute of Mining, Metallurgy and Petroleum Engineers, 177–190

Bukhari, S. W. H., Mohibullah, M., Khan, Kasi, A., and Iqbal, H., 2016. Biostratigraphy of the Eocene Nisai Formation in Pishin belt, Western Pakistan. *Journal of Himalayan Earth Sciences,* 49(1): 17

Choi, J. H., and Hariya, Y., 1992. Geochemistry and depositional environment of Mn oxide deposits in Tokoro belt, northeastern Hokkaido, Japan. *Economic Geology, 87*: 1265–1274

Crerar, D. A., Namson, J., Chyi, M. S., Williams, L., and Feigenson, I. M., 1982.Manganiferous cherts of the Franciscan assemblage: I. General geology, ancient and modern analogues, and implication for hydrothermal convection at ocean spreading centers. *Economic Geology,* 77: 519–540

Dasgupta, H. C., and Manickavasagam, R., 1981. Chemical and X-ray investigation of braunite from the metamorphosed manganiferous sediments of India. *NeuesJahrbuchfürMineralogie–Abhandlungen*, 142: 149–160.

Frakes, L., and Bolton, B., 1992. Effects of ocean chemistry, sea level, and climate on the formation of primary sedimentary manganese ore deposits. *Economic Geology*, 87: 1207–1217

Frenzel, G., 1980. The manganese ore minerals. In: Varentsov, I. M., Grasselly, G., (eds) Geology and geochemistry of manganese. Schweizerbart' scheVerlagsbuchhandlung, Stuttgart, 1, 25–158

Fernandez, A., and Moro, M. C., 1998. Origin and depositional environment of Ordovician stratiform iron mineralization from Zamora (NW Iberian Peninsula). *Mineralium Deposita,* 33: 606–619

Gultekin, A. H., 1998. Geochemistry and origin of the Oligocene Binkiliç manganese deposit, Thrace basin, Turkey. *Turkish Journal of Earth Sciences,* 7: 11–24

Gutzmer, J., and Beukes, N. J., 1997. Mineralogy and mineral chemistry of oxide facies manganese ores of the Postmasburg manganese field, South Africa. *Mineralogical Magazine,* 61: 213–231

Hein, J. R., Schulz, M. S., and Gein, L. M., 1992. Central Pacific cobalt rich ferromanganese crusts: historical perspective and regional variability. In: Keating, B. H., Bolton, B. R (eds) Geology and offshore mineral resources of the Central Pacific Basin. Springer-Verlag, Berlin, p 261

Hein, J. R., Yeh, H. W., Gunn, S. H., Gibbs, A. E., and Wang, C. H., 1994. Composition and origin of hydrothermal ironstones from central Pacific seamounts. *Geochimica et CosmochimiaActa,* 58: 179–189

Hein, J. R., Gibbs, A. E., Clague, D., and Torresan, M., 1996. Hydrothermal mineralization along submarine rift zones, Hawaii. *Marine Georesources and Geotechnology*, 14: 177–203

Hein, J. R., Koschinsky, A., Halbach, P., Manheim, F. T., Bau, M., Kang, J. K., and Lubick, N., 1997. Iron and manganese oxide mineralization in the Pacific. In: Nicholson, K., Hein, J. R., Buhn, B., Desgupta, S., (Eds.), Manganese Mineralization: Geochemistry and Mineralogy of Terrestrial and Marine Deposits. 119. *Geological Society Special Publication,* 123–138

Heron, A. M., and Crookshank, H., 1954. Directory of economic minerals of Pakistan. *Geological Survey of Pakistan Record,* 7:2

Jones, A.G., 1961. Reconnaissance Geology of Part of West Pakistan. A Colombo Plan cooperative project, Government of Canada, Toronto, 550.

Ingram, B. L., Hein, J. R., Farmer, G. L., 1990. Age determinations and growth rates of Pacific ferromanganese deposits using strontium isotopes. *Geochimica et Cosmochimica Acta,* 54:1709–1721

Jach, R., and Dudek, T., 2005. Origin of a Toarcian manganese carbonate: silicate deposit from the Krizna unit, Tatra Mountains, Poland. *Chemical Geology,* 224:136–152

Karakus, A., Yavuz, B., and Koc, S., 2010. Mineralogy and major-trace element geochemistry of the Haymana manganese mineralizations, Ankara, Turkey. *Geochemistry International,* 48:1014–1027

Kuhn, T., Bau, M., Blum, N., and Halbach, P., 1998. Origin of negative Ce anomalies in mixed hydrothermal-hydrogenetic Fe-Mn crusts from the Central Indian Ridge. *Earth and Planetary Science Letters,* 163:207–220

Lofti, M., Kahrazehi, M., and Majid, G., 2017. Geochemistry and origin of Dehoo manganese deposit, south Zahedan, southeastern Iran. *Arabian Journal of Geosciences*, 10:142

Meylan, M. A., Glasby, G. P., Knedler, K. E., and Johnston, J. H., 1981.Metalliferous deep-sea sediments. In Wolf, K. H., (ed) Handbook of strata-bound and stratiform ore deposits. Elsevier, Amsterdam, 9, 77–178

Mücke, A., Adjimah, K., and Annor, A., 1999. Mineralogy, petrography, geochemistry and genesis of the Paleoproterozoic Birimian manganese-formation of Nsuta/Ghana. *Mineralium Deposita,* 34: 297–311

Muan, A., 1959. Phase equilibria in the system manganese Oxide-Silica in air. American Journal of Science, 257, 297–315

Naseem, S., 1996. Genesis of manganese ore deposits of Lasbela area, Balochistan, Pakistan. [Dissertation]. University of Karachi, Pakistan. 259

Naseem, S., Sheikh, S. A., Mallick, K. A., 1997.Lithiophorite and associated manganese mineralization in Lasbela area, Balochistan, Pakistan. *Journal of Geosciences,* 1, 10–15

Nicholson, K., 1992. Contrasting mineralogical-geochemical signatures of manganese oxides: guides to metallogenesis. *Economic Geology,* 87: 1253–1264

Nicholson, K., Nayak, V. K., and Nanda, J. K., 1997. Manganese ores of the Ghoriajhor Monmunda area, Sundergarh District, Orissa, India: geochemical evidence for a mixed Mn source. In: Nicholson, K., Hein, J. R., Bühn, B., Dasgupta, S., (eds) Manganese mineralization: geochemistry and mineralogy of terrestrial and marine deposits. *Geological Society of London Special Publication,* 119:117–121

Oksuz, N., 2011. Geochemical characteristics of the Eymir (SorgunYozgat) manganese deposits, Turkey. Journal of Rare Earth, 29, 287–296

Oksüz, N., and Okuyucu, N., 2014. Mineralogy, geochemistry and origin of Buyukmahal manganese mineralization in the Artova ophiolitic complex, Yozgat, Turkey. *Journal of Chemistry,* 1–11

Ostwald, J., and Nayak, V. K., 1993. Braunite mineralogy and paragenesis from the Kajlidongri mine, Madhya Pradesh, 28. *Mineralium Deposita,* 153–156

Ozturk, H., 1993. Manganese mineralizations in Turkey: processes of formation and types. *Geological Engineering*, 43, 24–33 (in Turkish)

Panagos, A. G., and Varnavas, S. P., 1984. On the genesis of some manganese deposits from eastern Greece. In: Wauschkuhn, A., (ed).Syngenesis and epigenesis in the formation of mineral deposits. Spriger, Berlin, pp 553–561

Peters, T., 1988. Geochemistry of manganese-bearing cherts associated with Alpine-ophiolites and the Hawasina formations in Oman. *Marine Geology,* 84: 229–238

Polgári, M., Okita, PM.,and Hein, J. R., 1991. Stable isotope evidence for the origin of the Úrkút manganese ore deposit, Hungary. *Journal of Sedimentary Petrology,* 61, 384–393

Polgari, M., Hein, J. R., Vigh, T., Szabo-Drubina, M., Forizs, I., Biro, L., Muller, A., and Toth, A. L., 2012. Microbial processes and the origin of the Urkut manganese deposit, Hungary. *Ore Geology Reviews,* 47, 87–109

Rehman, S., 2019. Petrology of Ali Khanzai block of Zhob Ophiolite, Balochistan, Pakistan. [Dissertation]. University of Balochistan, Quetta. 78.

Roy, S., 1981. Manganese Deposits, Academic Press, London, p 458.

Roy, S., 1992. Environments and processes of manganese deposition. *Economic Geology,* 87, 1218–1236

Roy, S., Bandopadhyay, P. C., Perseil, E. A., and Fukuoka, M., 1990. Late diagenetic changes in manganese ores of the Upper Proterozoic Penganga Group, India. *Ore Geology Reviews,* 5: 341–357

Roy, S., 1997. Genetic diversity of manganese deposition in the terrestrial geological record. In: Nicholson, K., Hein, J. R., Buhn, B., Dasgupta, S., (eds). Manganese mineralization: geochemistry and mineralogy of terrestrial and marine deposits. *Geological Society of London Special Publication,* 119: 5–27

Sabatino, N., Neri, R., Bellanca, A., Jenkyns, H. C., Masetti, D., and Scopelliti, G., 2011. Petrography and high-resolution geochemical records of Lower Jurassic manganese rich deposits from Monte Mangart, Julian Alps. *Palaeogeography, Palaeoclimatology and Palaeoecology,* 299:97–109

Şaşmaz, A., Turkyilmaz, B., Oztürk, N., Yavuz, F., and Kumral, M., 2014. Geology and geochemistry of Middle Eocene Maden complex ferromanganese deposits from the Elazığ–Malatya region, eastern Turkey. *Ore Geology Reviews,* 56:352–372

Sengor, A. M. C., 1987. Tectonics of the Tethys sides: orogenic collage development in a collisional setting. *Annual Reviews Earth and Planetary Sciences,* 15: 213-244

Shah, M. T., and Khan, A., 1999. Geochemistry and origin of Mn-deposits in the Waziristan ophiolite complex, north Waziristan, Pakistan. *Mineralium Deposita,* 34: 697–704

Shah, M. T., and Moon, C., 2004. Mineralogy, geochemistry and genesis of the ferromanganese ores from the Hazara area, NW Himalayas, northern Pakistan (abs): 17th HKT International conference, Sikkim, India. *Journal of Asian Earth Sciences,* 23: 1–15

Sugisaki, R., 1984. Relation between chemical composition and sedimentation rate of Pacific Ocean floor sediments deposited since the middle Cretaceous: basic evidence for chemical constraints on depositional environments of ancient sediments. *Journal Geology,* 92:235–259

Toth, J. R., 1980. Deposition of submarine crusts rich in manganese and iron. *Geological Society of AmericaBulletin*, 91:44–54

Usui, A., and Nishimura, A., 1992. Submersible observations of hydrothermal manganese deposits on the Kaikata Seamount, Izu-Ogasawara (Bonin) Arc. *Marine Geology,* 106:203–216

Usui, A., and Someya, M., 1997. Distribution and composition of marine hydrogenetic and hydrothermal manganese deposits in the Northwest Pacific. In: Nicholson, K., Hein, J. R., Buhn, B., Dasgupta, S., (eds). Manganese mineralization: geochemistry and mineralogy of trrestrial and marine deposits. G*eological Society of London Special Publication,* 119:177– 198

Zarasvandi, A., Lentz, D., Rezaei, M., and Pourkaseb, H., 2013. Genesis of the Nasirabad manganese occurrence, Fars province, Iran: geochemical evidences. *Chemieder Erde-Geochemistry,* 73:495–508

Tables and Figures Captions

Table 1. Mineral chemistry of manganese minerals from Zhob manganese deposits.

Table 2. Whole rock major oxide (wt. %) and trace element (ppm) geochemical composition of manganese ore of the Zhob Ophiolite.

Table 3. Whole rock major oxide (wt. %) and trace element (ppm) geochemical composition of the host rocks ofZhob manganese deposits.

Table 4. Comparison between some major and trace element composition of the Zhob manganese occurrences and different types of manganese ores in the world.

Fig.1. Geological map showing (**a)** The study area, (**b)** Map of the Western Sulaiman Belt showing occurrences of the Zhob Valley Ophiolites and its surrounding rock units and (**c)** Map of Ali Khanzai block of the Zhob Ophiolite with the occurrences of manganese deposits (modified after Rehman, 2019; Siddiqi et al., 2016; Kakar et al., 2013; Bannert et al., 1992; HSC, 1960). BO; Bela Ophiolite, KO; Khanozai Ophiolite, MO; Muslim Bagh Ophiolite, WO; Waziristan Ophiolite, DO; Dargai Ophiolite, CO; Chilas Ophiolite, CF; Chaman Fault, PS; Penjwai Suture, HF; Herat Ophiolite,KB; Karakorum Block, MMT; Main Mantle Thrust, MBT; Main Boundary Thrust.

Fig.2. Field photographs showing (a) lenticular shape of manganese deposit surrounded by metachert, (**b)** layers of manganese surrounded by metacherts, (**c)** Mn-rich phases forming alternate bands with host metachert, and (**d)** massive manganese ore. Mn=manganese, Ch= metachert

Fig.3. Photomicrographs and micro-XRF scans showing (**a**) Braunite grains cross-cut by veinlets of quartz, (**b**) braunite enclosing pyrolusite forming a relic texture, (**c**) Pyrolusite micro-veins formed by filling of fractures and cracks in braunite and gangue minerals, (**d**) Massive pyrolusite grains showing fibrous sections, (**e**) Quartz in veinlets and well-developed crystals, filling vugs or interstitial spaces of manganese and iron minerals and (**f**) Barite filling cavities in manganese-rich phases. Note Fig (**b**) and (**f**) are micro-XRF images. Bra=Braunite, Pyr=pyrolusite, Hem=Hematite, Qz=Quartz.

Fig.4. Diagram of the ore paragenetic succession of the Zhob manganese deposits.

Fig.5. Diagrams showing comparison of **(a)** major oxides and **(b)** trace elements in Mn-rich, Fe-rich ores and host rocks.

Fig.6. (a) Bivariate plot of Si versus Al (Choi and Hariya, 1992) in which data points of the ore samples fall within the hydrothermal field. (**b)** Ternary plot of Fe-Mn-(Ni + Co + Cu) × 10 (Bonatti et al., 1972, modified by Toth, 1980) with the plotted data points within the hydrothermal field.

Fig.7. (a) Zn–Co–Ni diagram showing data for the manganese ores of Zhob, with fields for hydrothermal and hydrogenous deposits (after Choi and Hariya, 1992). (**b)** A plot of Co/Zn vs. Co+Ni+Cu for the manganese ores of Zhob (after Toth, 1980) and (**c**) TiO_2 vs Al_2O_3 diagrams of manganese ore samples.

Fig.8. Hypothetical model showing the geological environment of formation of the Zhob manganese deposits.

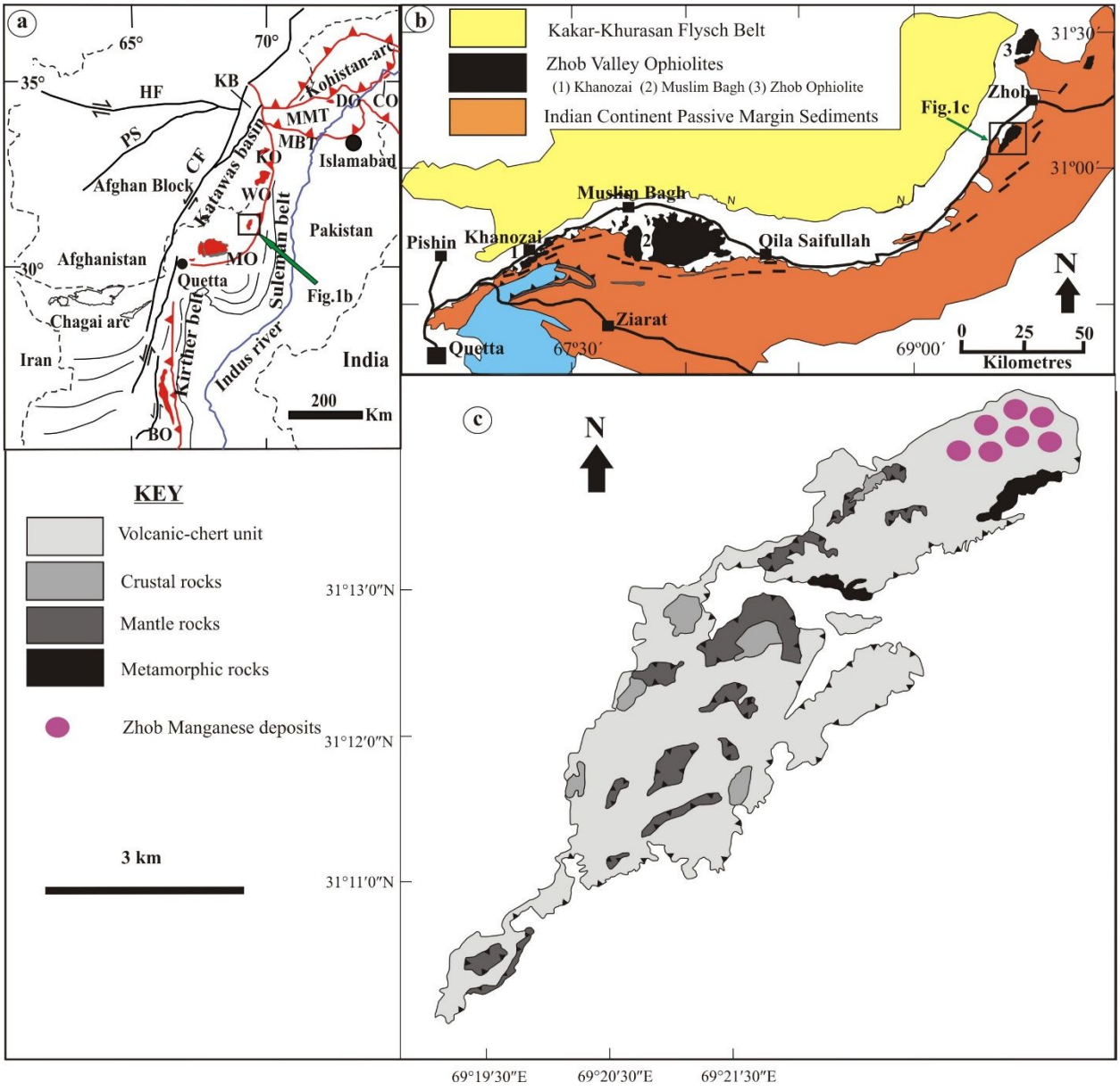
a
65°
70°
35°
HF
KB
Kohistan-arc
DO
CO
MMT
MBT
PS
CF
KO
Islamabad
Afghan Block
Katawas basin
WO
Pakistan
Sulemain belt
Afghanistan
30°
MO
Quetta
Fig.1b
Chagai arc
Kirther belt
Indus river
India
Iran
BO
200
Km
b
Kakar-Khurasan Flysch Belt
Zhob Valley Ophiolites
(1) Khanozai (2) Muslim Bagh (3) Zhob Ophiolite
Indian Continent Passive Margin Sediments
31°30′
3
Zhob
Fig.1c
31°00′
Muslim Bagh
N
Pishin
Khanozai
1
2
Qila Saifullah
Ziarat
Quetta
67°30′
69°00′
0
25
50
Kilometres
KEY
Volcanic-chert unit
Crustal rocks
Mantle rocks
Metamorphic rocks
Zhob Manganese deposits
3 km
c
N
31°13′0″N
31°12′0″N
31°11′0″N
69°19′30″E
69°20′30″E
69°21′30″E

Fig.1

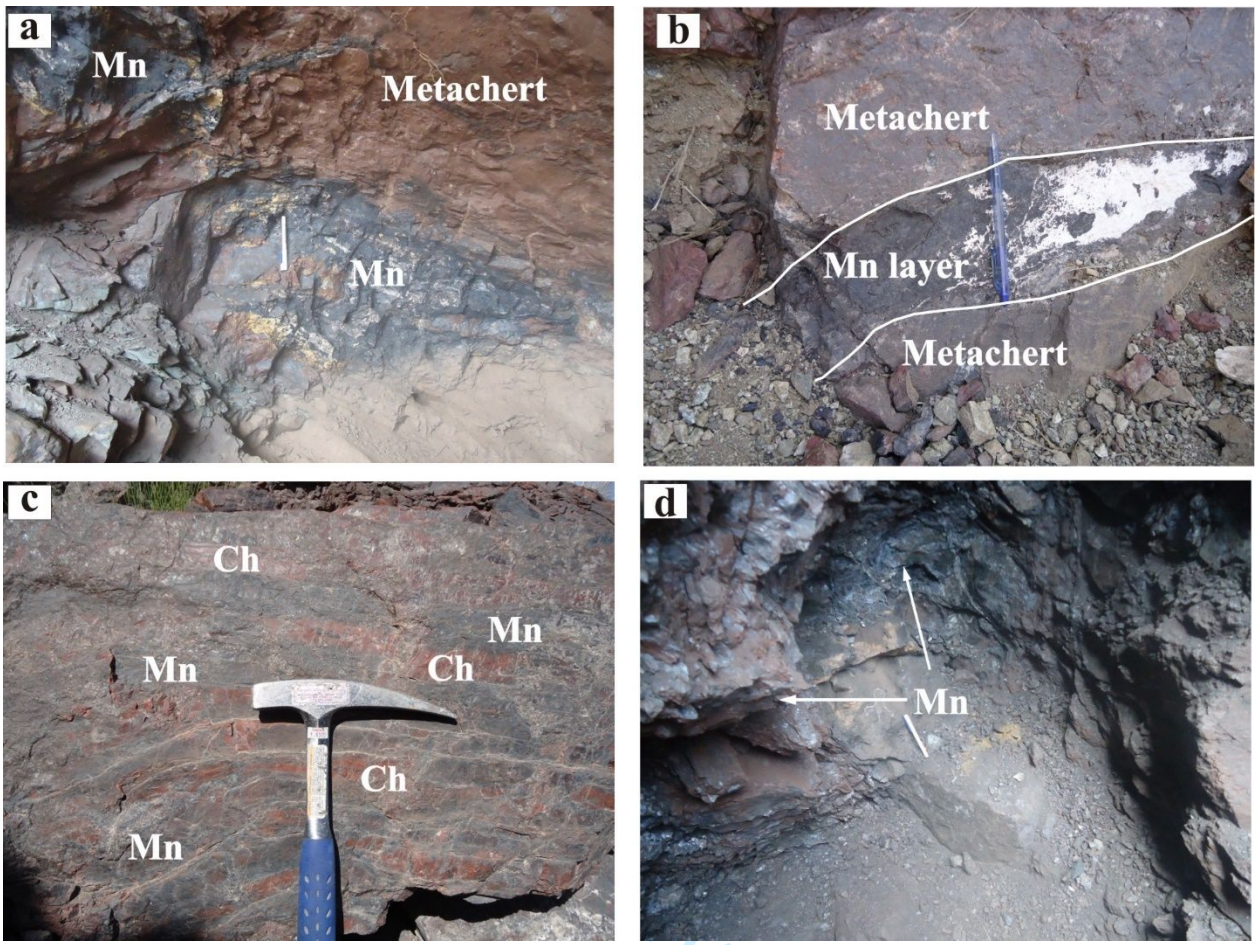

Fig. 2

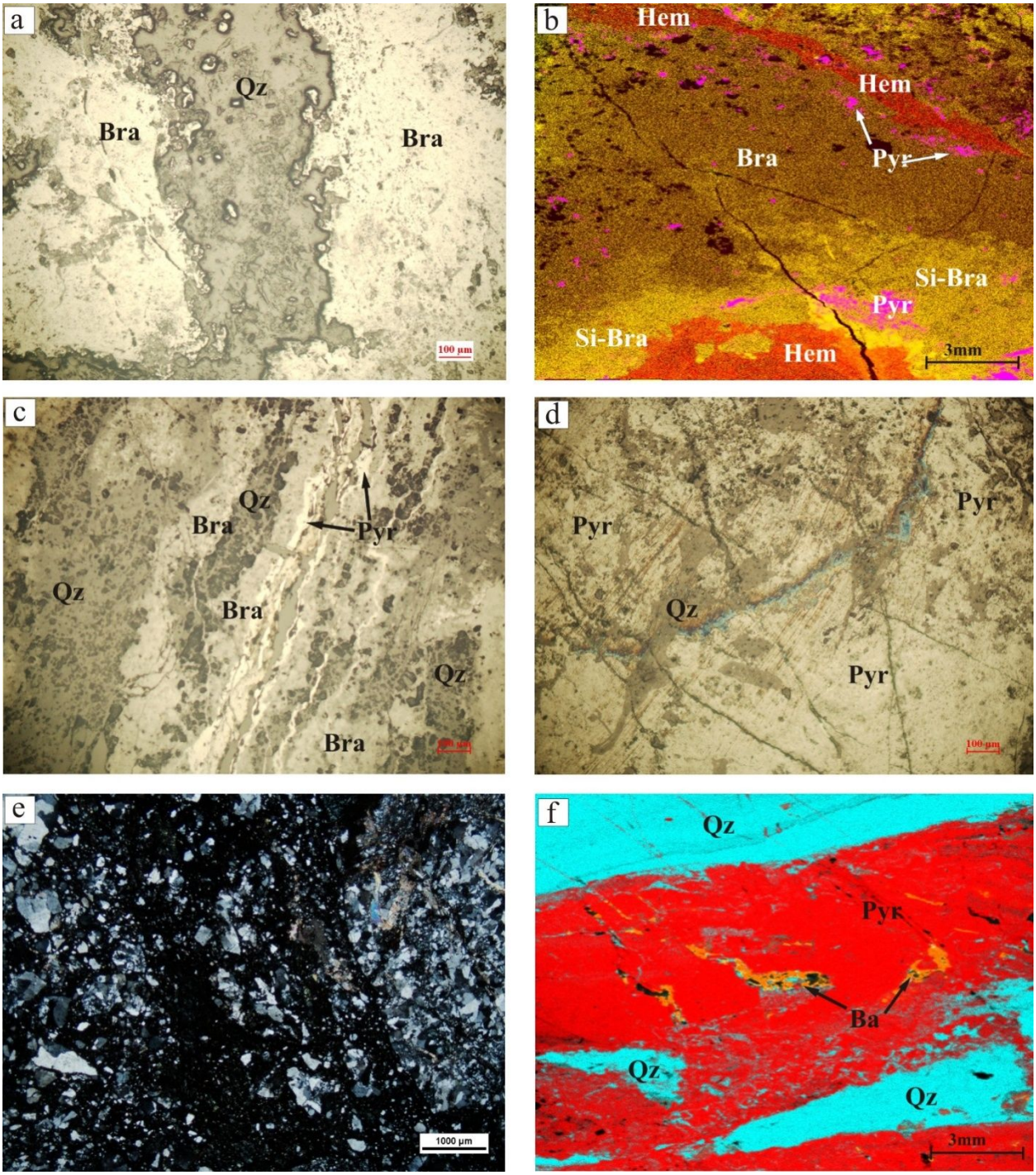
a
Qz
Bra
Bra
100 μm
b
Hem
Hem
Bra
Pyr
Si-Bra
Pyr
Si-Bra
Hem
3mm
c
Qz
Bra
Pyr
Qz
Bra
Qz
Bra
d
Pyr
Pyr
Qz
Pyr
100 μm
e
1000 μm
f
Qz
Pyr
Ba
Qz
Qz
3mm

Fig. 3

Ore minerals	Stages of ore mineralization		
	Early	Middle	Late
Pyrolusite	----------		----------
Braunite		----------	
Hausmannite			----------
Hematite			----------
Barite			----------
Silica gangue	----------	----------	----------

Fig. 4

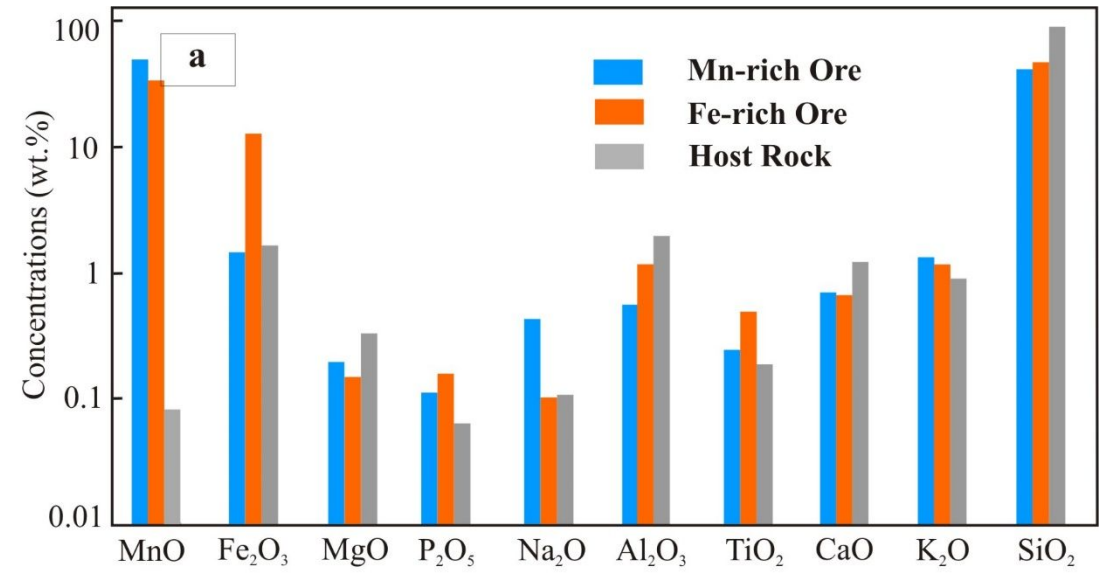
a
Mn-rich Ore
Fe-rich Ore
Host Rock
Concentrations (wt.%)
100
10
1
0.1
0.01
MnO
Fe2O3
MgO
P2O5
Na2O
Al2O3
TiO2
CaO
K2O
SiO2

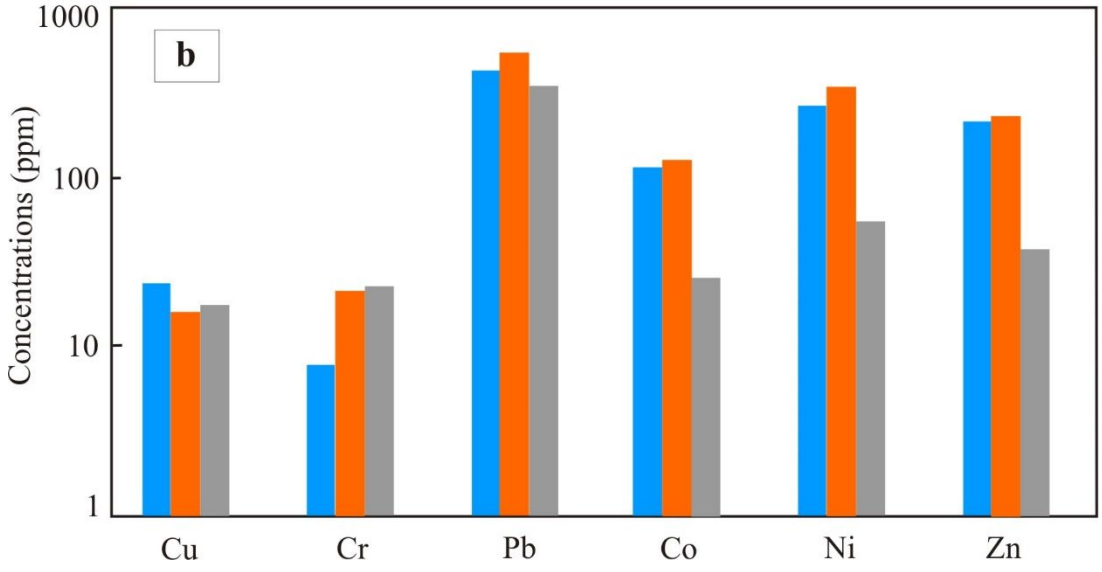
b
Concentrations (ppm)
1000
100
10
1
Cu
Cr
Pb
Co
Ni
Zn

Fig.5

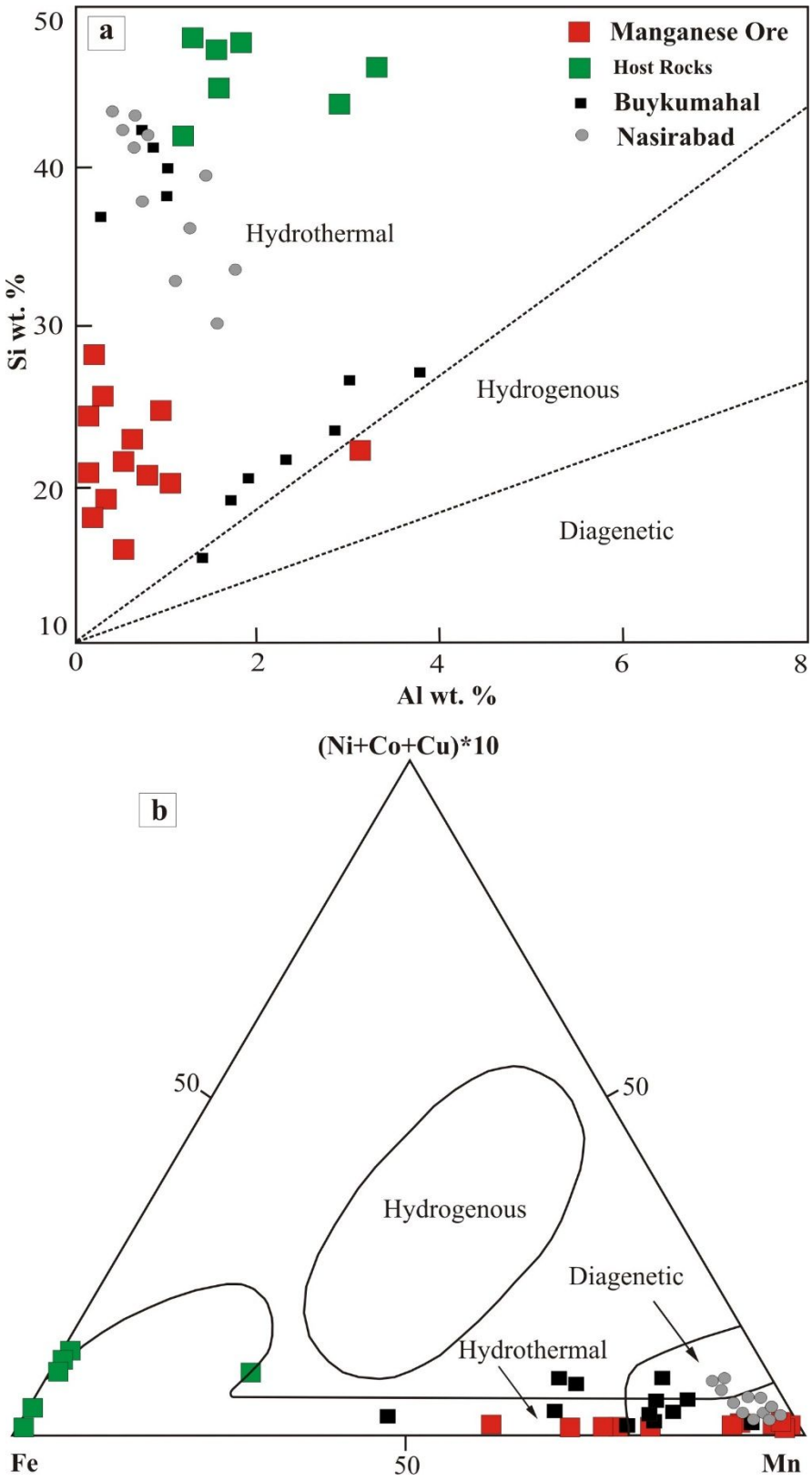
a
Manganese Ore
Host Rocks
Buykumahal
Nasirabad
Hydrothermal
Hydrogenous
Diagenetic
Si wt. %
Al wt. %
50
40
30
20
10
0
2
4
6
8
b
(Ni+Co+Cu)*10
50
50
Hydrogenous
Diagenetic
Hydrothermal
Fe
50
Mn

Fig.6

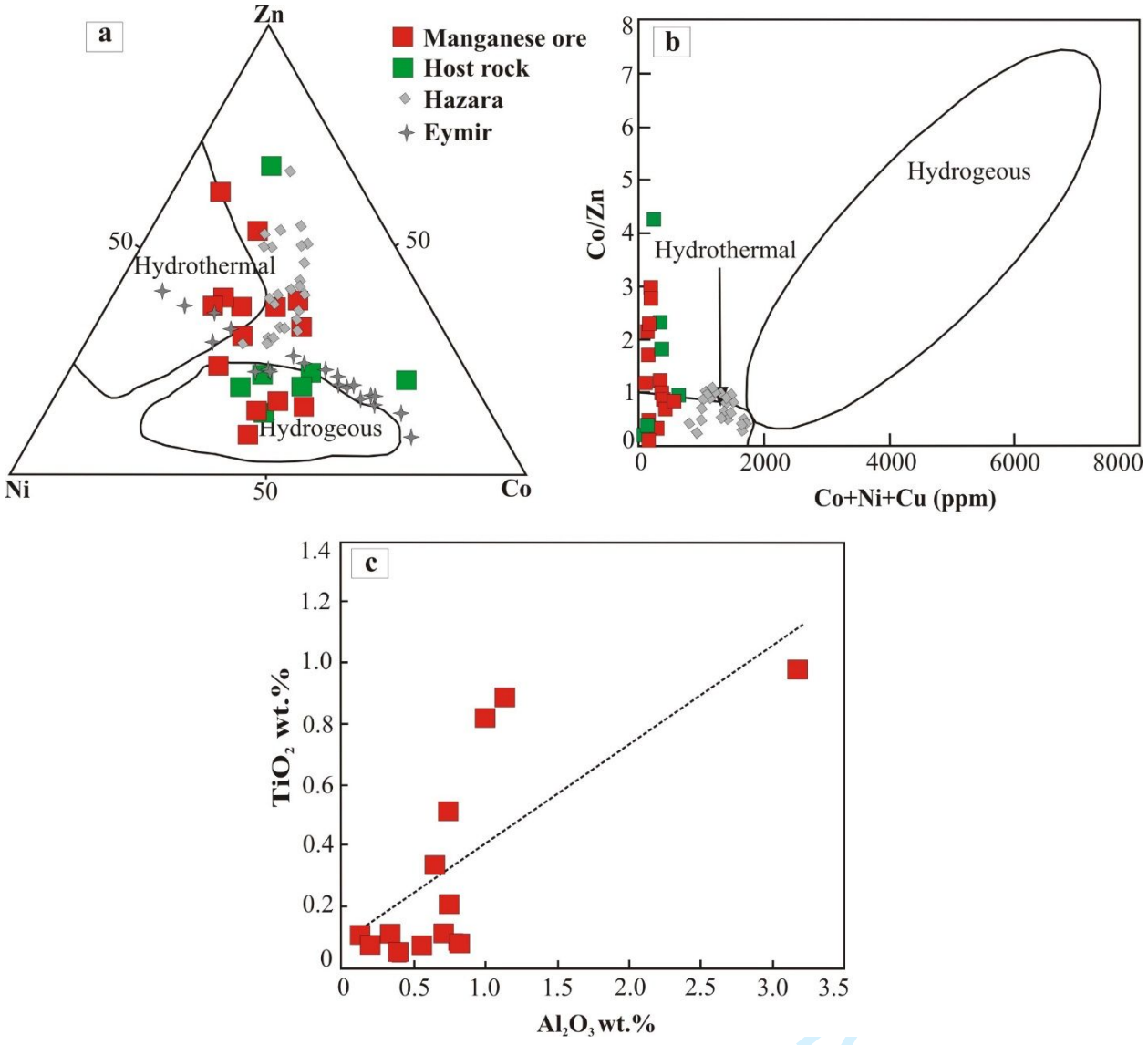
a
Zn
Ni
Co
50
50
50
Hydrothermal
Hydrogeous
Manganese ore
Host rock
Hazara
Eymir
b
Co/Zn
Co+Ni+Cu (ppm)
Hydrothermal
Hydrogeous
c
TiO2 wt.%
Al2O3 wt.%

Fig.7

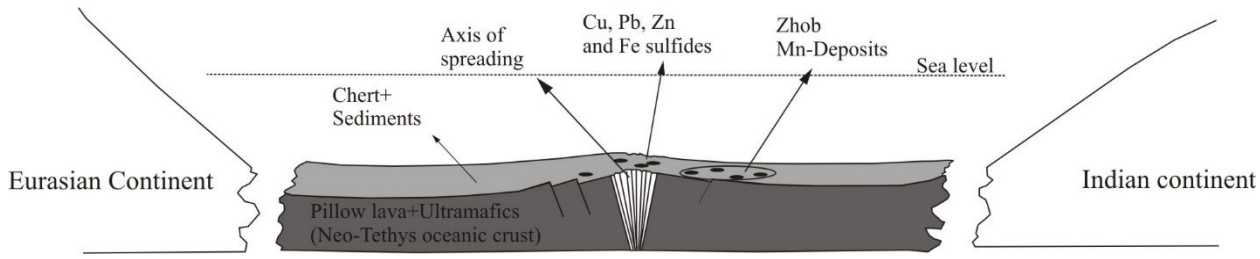
Axis of spreading
Cu, Pb, Zn and Fe sulfides
Zhob Mn-Deposits
Sea level
Chert+ Sediments
Eurasian Continent
Indian continent
Pillow lava+Ultramafics (Neo-Tethys oceanic crust)

Fig.8

Table 1. Mineral chemistry of manganese minerals of Zhob manganese deposits

Normal Braunite		Si-rich Braunite		Pyrolusite		Hematite		Barite	
SiO_2	13.02	SiO_2	28.41	SiO_2	bdl	SiO_2	bdl	CaO	2.98
Al_2O_3	1.46	Al_2O_3	1.18	Al_2O_3	dbl	TiO_2	1.62	SrO	0.85
Fe_2O_3	1.09	Fe_2O_3	0.85	Fe_2O_3	0.90	Al_2O_3	bdl	BaO	69.98
Mn_2O_3	82.19	Mn_2O_3	67.52	MnO_2	98.31	Fe_2O_3	89.27	MgO	bdl
MgO	0.29	MgO	0.43	MgO	0.00	Mn_2O_3	9.11	FeO	0.87
CaO	1.45	CaO	0.24	CaO	bdl	MgO	bdl	MnO	0.12
Na_2O	0.20	Na_2O	0.27	Na_2O	bdl	CaO	bdl	SO_3	25.05
K_2O	bdl	K_2O	bdl	K_2O	bdl	Na_2O	bdl	Total	99.85
Cr_2O_3	bdl	Cr_2O_3	bdl	Cr_2O_3	bdl	K_2O	bdl		
Total	99.75	Total	98.93	Total	99.24	Cr_2O_3	bdl		
						Total	100		

Detection Limit	
SiO_3	0.06
Al_2O_3	0.05
Fe_2O_3	0.10
Mn_2O_3	0.08
MgO	0.07
CaO	0.05
NaO_2	0.04
K_2O	0.05
Cr_2O_3	0.09
TiO_2	0.04
SrO	0.03
SO	0.08

Ions calculation based on 12 (O)		based on 2 (O)		based on 3 (O)		based on 4 (O)	
Si	1.54	Si	2.88	Si	0.00	Si	0.00	Ca	0.00
Al	0.20	Al	0.14	Al	0.00	Ti	0.04	Sr	0.01
Fe^{3+}	0.10	Fe^{3+}	0.06	Fe^{3+}	0.02	Al	0.00	Ba	1.03
Mn	8.21	Mn	5.80	Mn^{4+}	1.97	Fe^{3+}	1.89	Mg	0.00
Mg	0.05	Mg	0.07	Mg	0.00	Mn^{3+}	0.10	Fe	0.00
Ca	0.18	Ca	0.03	Ca	0.00	Mg	0.00	Mn	0.00
Na	0.05	Na	0.05	Na	0.00	Ca	0.00	S	0.99
K	0.00	K	0.00	K	0.00	Na	0.00		
Cr	0.00	Cr	0.00	Cr	0.00	K	0.00		

bdl=below detection limit

Table 2. Whole rock major oxides (wt. %) and trace elements (ppm) geochemical composition of manganese ore of Zhob manganese deposits

	Mn-Rich								Fe-Rich					
Sample	Z97b	ZA101	ZA102	Z103a	ZA104a	ZA104b	Z105b	Z106a	Z97a	Z105a	Z105M	Z108	ZA108b	Detection Limit
MnO	49.21	48.18	33.07	54.80	51.36	51.02	51.46	46.08	25.47	36.71	33.23	32.01	39.38	0.005
Fe_2O_3	0.31	4.36	3.19	1.16	1.76	0.13	0.83	0.09	16.83	8.95	13.98	10.7	12.5	0.005
MgO	0.3	0.44	0.09	0.11	0.26	0.12	0.08	0.16	0.15	0.05	0.14	0.24	0.19	0.005
P_2O_5	0.01	0.05	0.6	0.1	0.06	0.01	0.02	0.04	0.14	0.16	0.36	0.07	0.05	0.005
Na_2O	0.07	0.18	0.1	2.72	0.09	0.06	0.09	0.08	0.13	0.06	0.09	0.1	0.14	0.005
Al_2O_3	0.63	0.16	0.16	0.56	0.33	0.8	1.08	0.71	0.37	0.73	3.21	1.01	0.63	0.005
TiO_2	0.53	0.07	0.1	0.08	0.12	0.07	0.91	0.11	0.07	0.21	0.97	0.84	0.34	0.005
CaO	0.06	1.44	0.05	0.52	1.81	0.26	bdl	1.44	0.02	0.01	1.39	0.35	1.59	0.005
K_2O	1.38	1.72	1.23	1.83	0.85	1.08	1.23	1.31	1.08	1.08	1.23	1.38	1.08	0.005
SiO_2	43.21	36.5	55.11	32.37	39.19	41.84	41.01	47.44	49.6	51.2	43.95	49.68	42.05	0.005
LOI	4.35	6.20	5.30	5.50	3.30	4.40	3.50	2.55	5.50	0.90	3.15	3.80	1.20	
Total	100.06	99.30	99.00	99.75	99.13	99.79	100.21	100.01	99.36	100.06	101.70	100.18	99.15	
Mn	38.11	37.31	25.61	42.43	39.77	39.51	39.85	35.68	19.72	28.43	25.73	24.79	30.50	
Fe	0.22	3.05	2.23	0.81	1.23	0.09	0.58	0.06	11.77	6.26	9.78	7.48	8.74	
Mn/Fe	176	12.24	11.48	52.30	32.31	435	69	567	1.68	4.54	2.63	3.31	3.49	
Cu	43	17.2	5.2	39	8	45	3.6	25	36.4	10	23.2	3.2	7	0.05
Cr	bdl	29.8	bdl	8.4	3.2	9.6	8	3	41.2	16	4	18.8	26	0.05
Pb	305	706	558.2	29	410	212.4	687	484.4	378	687.4	647	546.2	390.2	0.05
Co	85.2	21	105	179	168.2	185	124	90	80.2	140	231	131	90.4	0.05
Ni	313.4	132.2	314.6	198.6	379.4	344.4	147	219.6	333.6	403	437.4	287	239.8	0.05
Zn	175	163.2	250	305	184.2	240	320	145	161	394.2	408.2	141	115.4	0.05
Co/Zn	0.49	0.13	0.42	0.59	0.91	0.77	0.39	0.62	0.50	0.36	0.56	0.93	0.78	
Co/Ni	0.27	0.16	0.33	0.90	0.44	0.54	0.51	1.59	0.24	0.35	0.53	0.46	0.38	

LOI=Loss of Ignition, bdl=below detection limit

Table 3. Whole rock major oxides (wt. %) and trace elements (ppm) geochemical composition of host rocks of Zhob manganese deposits

Sample	Z97H	Z97aH	Z104H	ZA106	Z111H	ZA112	Z113H	Detection Limit
MnO	0.01	0.51	0.01	0.01	0.01	0.01	0.01	0.005
Fe_2O_3	1.33	1.30	2.34	1.13	2.02	2.13	1.11	0.005
MgO	0.11	0.08	0.12	0.14	1.42	0.22	0.23	0.005
P_2O_5	0.03	0.01	0.34	0.01	0.02	0.01	0.02	0.005
Na_2O	0.08	0.14	0.04	0.05	0.15	0.15	0.14	0.005
Al_2O_3	1.58	1.75	1.23	1.54	1.39	3.29	2.91	0.005
TiO_2	0.09	0.08	0.08	0.50	0.07	0.27	0.24	0.005
CaO	0.62	0.46	4.11	0.06	0.20	1.65	1.52	0.005
K_2O	0.64	0.51	1.23	1.31	0.77	0.93	0.94	0.005
SiO_2	88.43	93.11	84.18	93.83	93.40	91.03	87.63	0.005
LOI	7.25	1.90	5.90	1.95	0.60	0.95	5.90	
Total	100.17	99.85	99.58	100.53	100.05	100.64	100.65	
Mn	0.01	0.39	0.01	0.01	0.01	0.01	0.01	
Fe	0.93	0.91	1.64	0.79	1.41	1.49	0.78	
Mn/Fe	0.01	0.43	0.01	0.01	0.00	0.01	0.01	
Cu	46	21.20	26.20	6.40	5	7	13.00	0.05
Cr	34.00	16	5.20	12.00	41.40	33.40	15	0.05
Pb	193	397	302.40	390.40	322.20	316	435.20	0.05
Co	19.20	26.40	45	24.40	37.20	6	23.40	0.05
Ni	18.40	88.20	74	83.40	39	6	66.40	0.05
Zn	30	27	60	38	47	27	40	0.05
Co/Zn	0.64	0.98	0.75	0.64	0.79	0.21	0.59	
Co/Ni	1.04	0.30	0.61	0.29	0.95	0.97	0.35	

Table 4. Comparison between some major and trace element composition of the Zhob manganese occurrences and different type of manganese ores in the world

Country	Iran	Turkey	Pakistan	Turkey	Turkey	Japan
Ore deposit	Dehoo (1)	Cayirli (2)	Wazirstan (3)	Ulukent (4)	Binkilic (5)	Honde (6)
Origins	hydrothermal	Hydrothermal	Hydrothermal	Sedimentary	Sedimentary	Hydrogenous
SiO_2	25.87	63.02	43.69	13.6	10.65	12.67
TiO_2	0.04	0.03	0.32	0.1	0.02	0.04
Al_2O_3	1.07	0.65	0.73	2.49	2.85	1.27
Fe_2O_3	2.44	0.68	2.96	3.72	2.46	0.59
MnO	45.59	29.22	45.88	63.78	33.39	67.21
MgO	0.42	0.2	0.6	1.99	1.27	0.08
CaO	5.17	0.24	1.28	4.05	18.96	1.67
Na_2O	0.12	0.05	0.29	0.24	0.39	0.07
K_2O	0.21	0.11	0.22	0.05	0.56	0.46
P_2O_5	0.08	0.04	0.25	0.18	0.31	0.12
Cr	(-)	13.7	45	(-)	26	16
Co	28.75	25.21	11	13	59	222
Ni	89.13	69.4	36	10	167	341
Cu	62.13	154.9	72	56	26	691
Zn	77.74	66.6	64	70	49	147
Pb	19.68	6.5	49	65	(-)	18
Mn/Fe	56.23	97.17	199	18.98	15.03	133.43
Co/Zn	0.38	0.38	0.17	0.19	1.2	1.51
Co/Ni	0.33	0.36	0.31	1.3	0.35	0.65

Table 4 *continue*

Pakistan	Turkey	Iran	Turkey	Pakistan
Hazara (7)	Eymir (8)	Nasirabad (9)	Buyukmahal (10)	Zhob (This Study)
Hydrothermal-Hydrogenous	Hydrothermal-Hydrogenous	Hydrothermal-Hydrogenous	Hydrothermal-Hydrogenous	Hydrothermal
9.41	16.04	84.39	49.62	44.09
0.84	0.02	0.06	0.16	0.34
12.53	0.73	1.29	3.66	0.80
20.33	0.26	0.76	6.63	5.75
33.78	69.91	8.82	26.79	42.46
0.59	0.59	0.3	1.31	0.18
6.43	0.24	0.5	2.94	0.69
0.07	0.01	0.17	0.18	0.30
0.88	0.05	0.2	0.67	1.27
3.73	0.07	0.02	0.11	0.13
247	(-)	(-)	(-)	29.85
404	103.5	85.36	367.4	125.24
305	67.35	86.13	280.4	288.46
375	80.5	117.74	450.8	28.05
580	62.45	35.62	81.8	230.67
2357	9.33	2.02	25.8	541.6
2.16	880.33	18.85	6.06	105.37
0.7	2.24	2.2	4.49	0.57
1.32	1.54	0.99	1.31	0.51

Analysis after (1) =Lofti et al. (2017), (2) =Karakus et al. (2010), (3) =Shah and Khan (1999), (4) =Ozturk (1993), (5) =Gultekin (1998), (6) =Choi and Hariya (1992), (7) =Shah and Moon (2004), (8) =Oksuz (2011), (9) =Zarasvandi et al. (2013), (10) =Oksuz and Okuyucu (2014)